

An ATHOS3 Code Model Development and Fluid-Elastic Vibration Analysis for YGN 3/4 Steam Generators

Ukhwan Sur*

(Received August 28, 1997)

This paper provides a combined thermal hydraulic and vibration analysis of the Yonggang Nuclear (YGN) 3/4 steam generators using a developed ATHOS3 code model to calculate the multi-dimensional two-phase flow distribution, and ANSYS code to calculate the free and forced responses of a specific U-tube. The local porosity idea has been used for the ATHOS3 step 1 model development and the flow-induced vibration. The step 2 model development in the tube lane region was carried out to change into rectangular modes which separated the hot and cold sides of inverted U-tubes and to enhance understanding of the difference between ATHOS3 and Flow 3 modeling. Stability ratios for the tube vibration has been calculated using the developed ATHOS3 model and ANSYS code. The results of this analysis for YGN3/4 steam generators show that the design goals were met for all three critical regions of cross flow, with the stability ratios much less than 1.0.

Key Words: Fluid-Induced Vibration, Finite Element, Steam Generator, Elastic Vibration Analysis, Dynamic Characteristics, Thermal Hydraulic Analysis, Modified ATHOS3 Code, Stability Ratio

1. Introduction

PWR (Pressurized Water Reactor) recirculating steam generators are essentially large shell and tube heat exchangers that transfer thermal energy from the higher pressure primary circuit to the secondary turbine circuit. The energy transfer occurs across thousands of thinwalled inverted U-tubes contained within the shell.

It is imperative to maintain the integrity of these tubes since they provide the main barrier between the radioactive primary fluid and the inactive secondary fluid. The failure of a single tube can force a plant shut down which can cost several hundred thousand dollars per day in lost power production alone.

Tube damage can result from various corrosion processes as well as from fretting wear and high cycle fatigue. Fretting wear and fatigue failure of tubes generally result from the excessive flow

-induced vibration of inadequately-supported tubes in regions of cross-flow such as U-bends, preheater compartments and in front of down-comer windows. These types of failures are less common than corrosion-related ones (Tatone and Pathania, 1984). Nevertheless, in view of high shut down and repair costs, there is still a high incentive to avoid flow-induced vibration-related tube failure.

Damaging flow-induced vibration can be prevented by providing an adequate number of support points along the tubes and by designing support configurations to have the lowest possible tube/tube support clearances. The number and location of tube supports can be determined a priority by conducting a thorough flow-induced vibration analysis at the design stage.

In a typical inverted U-tube steam generator of the type found in the majority of PWR nuclear power plants, there are, for vibrational assessment purposes, three types of shell side flows. In the first, bundle entrance flow is composed of either subcooled or saturated water of high density

* Halla Institute of Technology

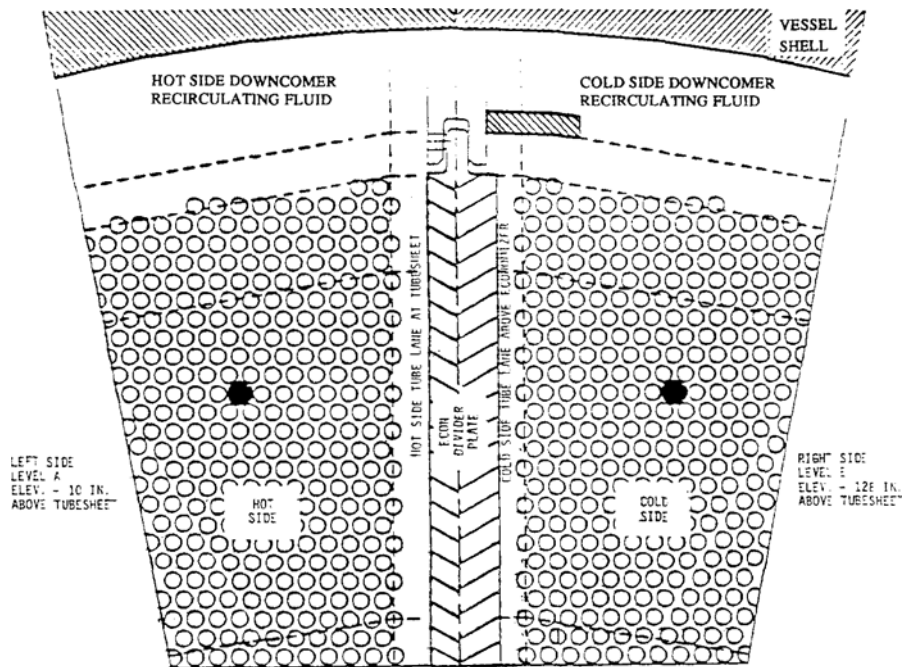


Fig. 1 Plan view of analysis model at left side elev. - 10 in. above tubesheet.

which enters the lower type bundle in cross-flow at various orientations to the pattern of the tube array. In the second, bundle exit flow is composed of a water and steam mixture traveling in a more or less vertically upward direction and subjecting tube spans in the upper region which are normally not as well supported as tube spans in the entrance region. The third type, shell side flow, is axial flow, which does not possess nearly as much potential for exciting tube spans as cross flow. Therefore, it has not been included as a subject of this study.

The "Special Report," of Combustion Engineering, "Flow Induced Vibration Analysis of Yonggwang Nuclear(YGN) 3/4 Steam Generator Economizer and Lower Tube Bundle Region" (Beard, 1988), utilized a two step flow distribution analysis methodology for predicting secondary side fluid velocities in the vicinity of the tube lane. First, thermal hydraulic analysis of the entire steam generator is performed using the ATHOS3 Code(Singhal, 1982). Second, using ATHOS3 results for boundary conditions, the lower tube bundle region near the tube lane is analyzed using the FLOW3 Code(Hiestand and

Thakkar, 1984). There were considerable differences in local velocities calculated by the two codes. These differences are mainly because of different modeling techniques of the two codes.

The focus of the study presented in this paper is the "tube lane" region(Figure 1), where due to lack of flow resistance, the fluid velocities are higher than within the compact tube bundle. The tube lane has a rectangular shape, while the ATHOS3 code models the steam generator using the polar coordinate system, which is consistent with the overall steam generator geometry. The ATHOS3 code can not model the rectangular tube lane region without tubes accurately. In order to access fluid velocities in the "tube lane" region more accurately than available from the ATHOS3 analysis, the code is modified for the "tube lane".

2. Development of ATHOS3 Code Model and Flow Distribution Analysis

Differences in ATHOS3 and Flow 3 calculated velocities in the vicinity of the open tube lane and annulus region are partly because of different

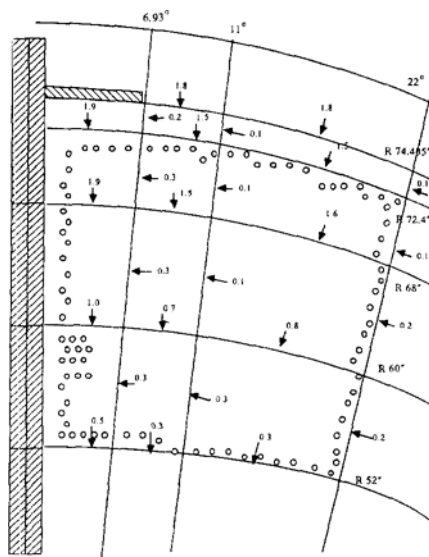


Fig. 2 Fluid velocities at the cold side downcomer entrance level (Reference ATHOS3 analysis).

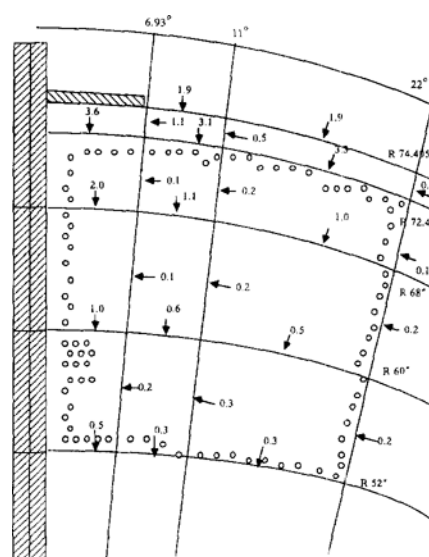


Fig. 3 Fluid velocities at the cold side downcomer entrance level (Modified step 1 analysis).

modeling approaches of the two codes. The ATHOS3 code utilizes average porosity of the two adjacent nodes to compute cell face areas and it also uses a finite difference grid based on the polar coordinate system to represent a rectangular tube lane. The Flow 3 code employs a network representation of the flow field. Hence it models the details of the steam generator geometry more accurately.

The “developed” ATHOS3 analysis is accomplished in two steps. The intermediate Step 1 analysis consists of using local porosity to calculate the radial direction flow areas at the tube bundle/annulus interface. The Step 2 analysis includes a model of the rectangular tube lane.

2.1 The step 1 model development and flow distribution analysis

The ATHOS3 computes the cell face area porosity by taking the arithmetic mean of the volumetric porosity of two adjacent cells. This method reduces sensitivity of area porosity value due to grid selections. It may generate unrealistic local results at the tube bundle boundaries without affecting overall results.

The radial and circumferential velocities at the

cold side downcomer fluid entrance level are illustrated in Fig. 3. The velocities in the annulus increased reflecting the effect of lower radial cell face area porosities. The maximum velocity for this model is 3.6ft/sec compared to 1.9ft/sec for reference analysis shown in Fig. 2. The velocities in the tube lane nodes are also higher; the maximum velocity is 2.0ft/sec vs. 0.9ft/sec for the reference case.

2.2 The step 2 model development and flow distribution analysis

The finite difference grid based on the polar coordinate system is appropriately used by the ATHOS3 model to analyze the YGN 3/4 steam generator. The steam generator includes an open rectangular lane separating the hot and cold sides of inverted U-tubes. The local characteristics in the lane are influenced by the absence of tube bundle friction. It is difficult to isolate and study these characteristics with the model based on the polar coordinate system. As demonstrated by Fig. 2, the 6.93° circumferential boundary includes both the open lane and some tubes in the node. With the porous media concept of ATHOS 3, the properties of the open tube lane and tube bundle regions are combined and nodes with higher

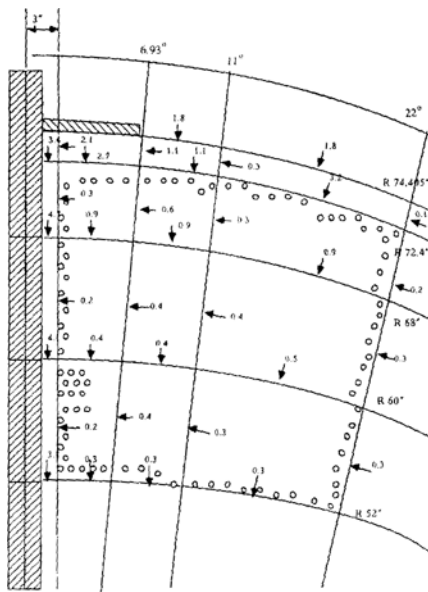


Fig. 4 Fluid velocities at the cold side downcomer entrance level (Modified step 2 analysis).

porosity and less heat transfer and friction surfaces than the tube bundle nodes are generated for analysis.

The Step 2 modifications are incorporated in the geometry preprocessor and a new data file is created for use by the thermal hydraulic module. The radial and circumferential velocities at the cold side downcomer entrance level are plotted in Fig. 4. The figure demonstrates the influence of geometry on local flow distribution. The maximum velocity in the annulus increases from 1.9ft/sec for the reference case(Fig. 2), to 3.2ft/sec for the Step 2 analysis. The maximum velocity in the tube lane correspondingly increases from 0.9ft/sec to 4.7ft/sec. The maximum velocities calculated by the Flow 3 model(Fig. 5) are 7.1ft/sec in the annulus and 15.2ft/sec in the tube lane.

The "developed" ATHOS3 Code analysis of the YGN 3/4 steam generators are performed to demonstrate that the "developed" ATHOS3 code would predict reasonable and consistent velocities, when compared with FLOW3, provided sufficiently detailed modeling of the tube lane and annulus region is incorporated into the ATHOS3 normalization.

Therefore, this model ends up with realistic

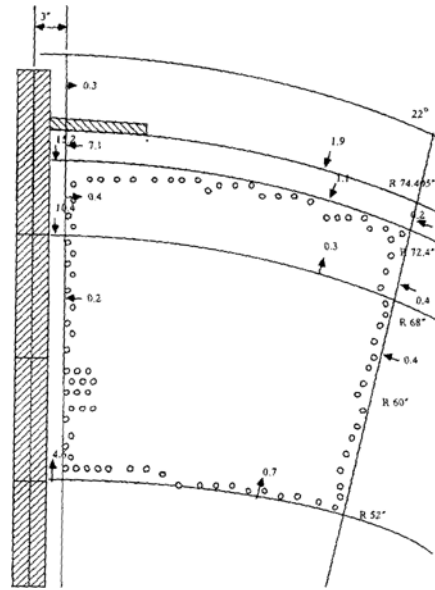


Fig. 5 Fluid velocities at the cold side downcomer entrance level (FLOW3 analysis).

results comparing with the FLOW3 model.

3. Tube Vibration Evaluation

The ASME code, Section III Design Analysis report for the YGN 3/4 steam generators will include an evaluation of tube vibration at all critical locations for the entire tube bundle configuration while this paper is limited in scope to the economizer and lower tube bundle region.

A vibration analysis on the YGN 3/4 steam generator tubes and tube supports configuration to obtain information required to evaluate the fluid elastic instability phenomena was performed. ANSYS, a general purpose computer program(1992), was used to perform a finite element modal analysis.

3.1 Geometry

A single tube in row 1 is modeled in this study and is supported at various locations by partial eggcrates, full eggcrates and a cold side flow distribution plate in addition to the tube sheet. Figure 6 shows the tube support arrangement for YGN 3/4 steam generators. Eggcrates and the

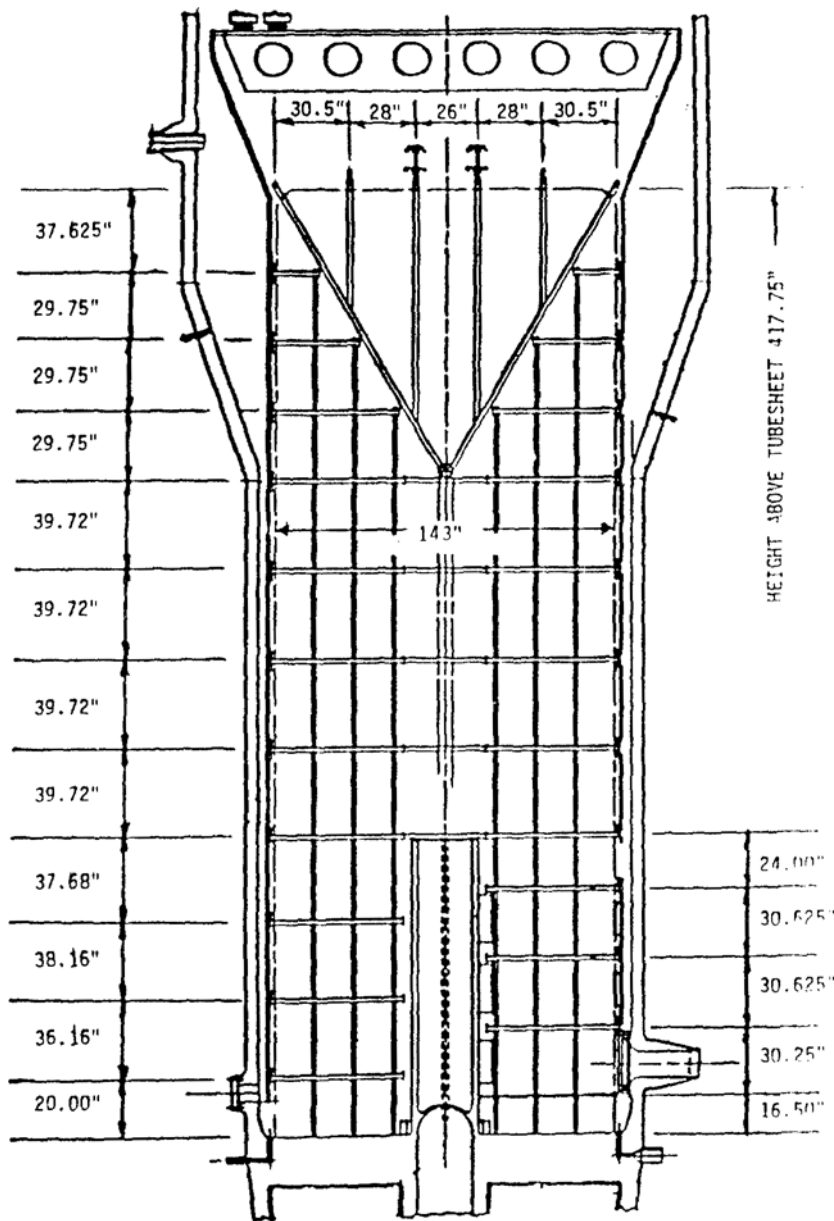


Fig. 6 Tube supports arrangement YGN 3/4 steam generator.

flow distribution plate are assumed to provide simple support to tube lateral motions while the tube sheet effectively restrains the rotational and translational motions.

3.2 Finite element model and eigenvalue analysis

The finite element model (FEM) is composed

of 122 structural pipe elements defined by 123 nodes with mass characteristics calculated from the mass equation described above. Flow distribution evaluations performed in Section 2.2 determine primary and secondary fluid density data for this purpose. A schematic of tube row 1 is shown in Fig. 7 with support locations identified by node numbers used in the FEM analysis. The

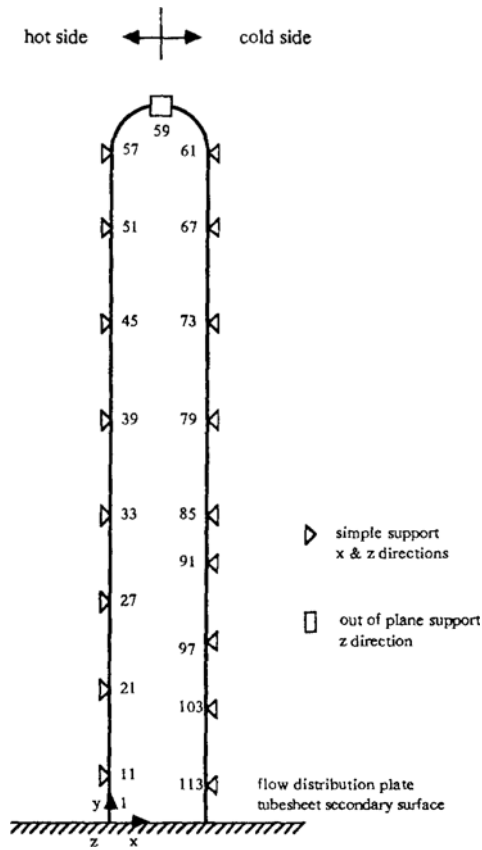


Fig. 7 ANSYS model for YGN 3/4 steam generator (Tube row 1).

modulus of elasticity for each element is assumed constant, 28.7×10^6 psi, and is based on a conservative average tube operating temperature of 600°F at 100 percent power for row number one.

Figure 8 provides a composite description of the cross flow velocity distribution and pertinent mode shapes for YGN 3/4 steam generator tubes on the cold side. Assessment of modes most likely to be excited by cross flow and produce damaging vibrations is enhanced by this data format.

An eigenvalue analysis determines the mode shape and natural frequencies for the tube model described above. The first seventeen modes of vibration vary in frequency from 35.4 to 281 Hz. Figure 9 contains the three modes of interest regarding flow induced vibration assessment. Modes 15, 16 and 17 exhibit maximum response in the regions of flow at the cold side recirculation

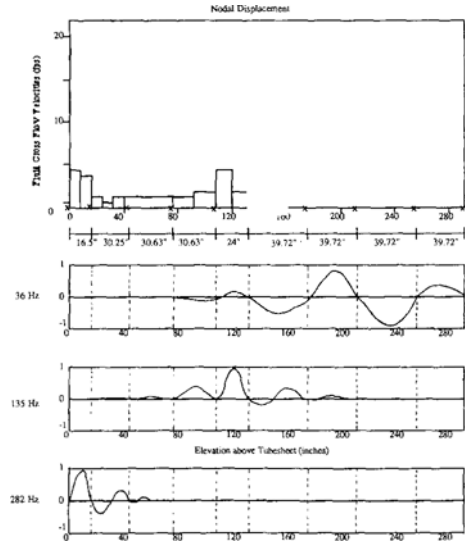


Fig. 8 Comparison of cross flow velocities with modal displacements and frequencies. (Cold side tube lane).

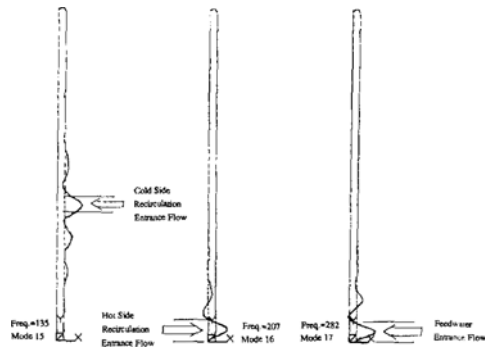


Fig. 9 Mode shapes for YGN 3/4 steam generator (tube row 1).

tion entrance, hot side recirculation, and feedwater entrance to the tube bundle, respectively. These modes will be evaluated in the following section with regard to effective and critical velocity leading to a determination of stability margins against potentially damaging vibrations.

Normally tubes in a heat exchanger are subjected to fluid cross-flow. There exists a threshold velocity where the onset of fluid-elastic unstable vibrations occur. This is defined as the critical velocity and is given by equation (Connors, 1980)

$$V_{cr} = f_n k d \sqrt{M_o \delta_o / (\rho_o d^2)} \quad (1)$$

where

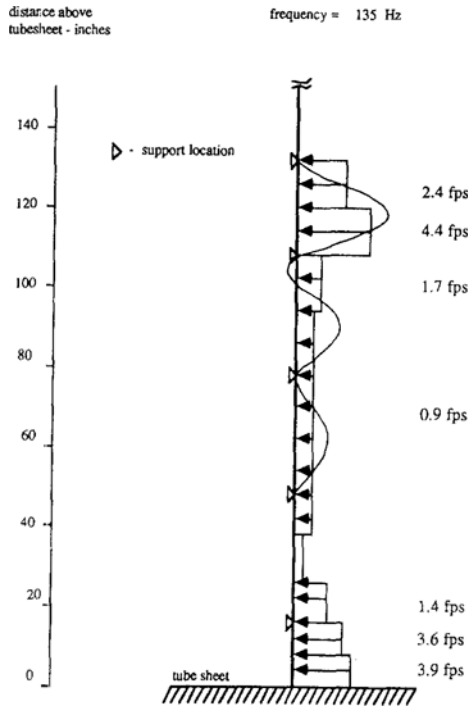


Fig. 10 Model for YGN 3/4 cold side downcomer entrance tube bundle corner region.

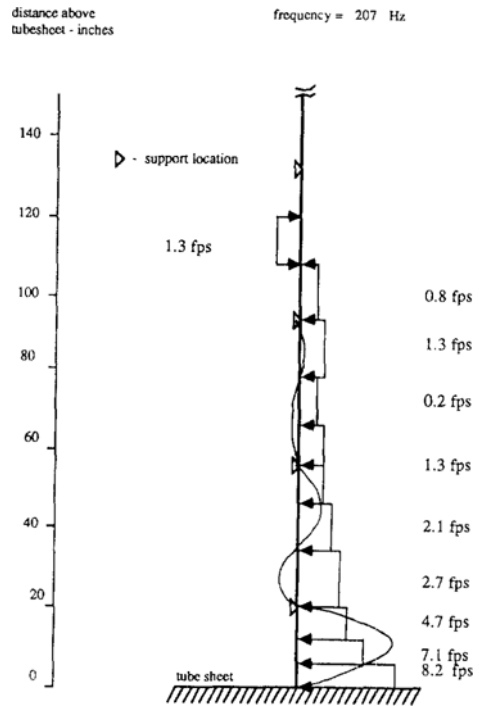


Fig. 12 Model for YGN 3/4 hot side flow in the tube lane.

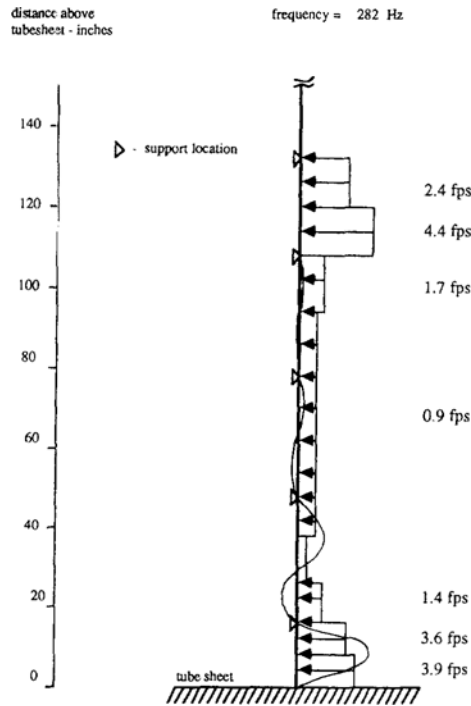


Fig. 11 Model for YGN 3/4 cold side feedwater flow distribution in the tube lane.

f_n = Natural Frequency of nth Mode of Vibration (Hz)

k = Threshold Instability Constant (Dimensionless)

d = Tube O. D. (in.)

M_o = Reference Mass of Tube per Unit Length lb-sec²/in²

δ_o = Logarithmic Decrement = $2\pi\xi$

ξ = Damping Ratio of Tube in Fluid

ρ_o = Reference Fluid Density lb-sec²/in⁴

If the cross-flow occurs over a partial span or only one span of a multiplan tube, the effective velocity must be determined since the critical velocity is greater for partial than full span flow. Reference (Connors, 1980) presents a method for determining this value which is denoted by the term, V_{eff} .

The general equation (Connors, 1980) for this evaluation is given by

$$V_{eff}^2 = \frac{\int^{flow} \frac{\rho(x)}{\rho_o} V(x)^2 \phi(x)^2 dx}{\int^{total} \frac{M(x)}{M_o} \phi(x)^2 dx} \quad (2)$$

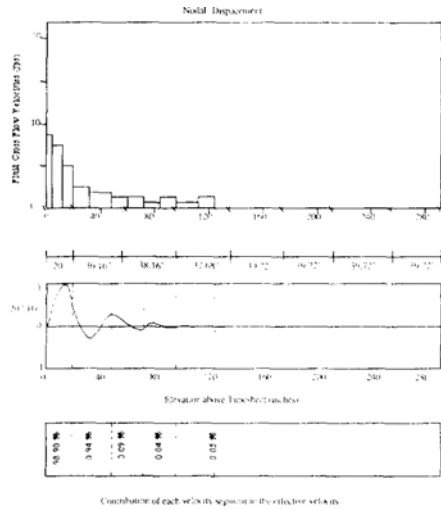


Fig. 13 Relationship between effective velocity and modal displacements.

where the upper integral is evaluated over the flow region and the lower integral over the complete tube span.

Critical velocity calculations for YGN3/4 at three critical regions of highest cross-flow, the cold side downcomer entrance, feedwater entrance flow, and hot side downcomer entrance above the tube sheet were performed. Vibration mode shapes and natural frequencies utilized in the evaluation of V_{cr} are shown in Fig. 9. Cross-flow velocity distributions presented in Figs. 10 through 12 are used to evaluate the effective velocities, V_{eff} , and are obtained from the flow distribution analysis results of Sec. 2.2. Figure 13 is provided as an example of the relative contribution of each span modal displacement to the total effective velocity calculation.

4. Results and Conclusions

The developed ATHOS3 model flow distribution analyses. Step 1 and 2, demonstrate that representative local velocities can be obtained with the ATHOS3 code provided sufficiently detailed modeling is used.

A summary of vibration analysis results is presented in Table 1. YGN 3/4 is evaluated at three critical regions of cross flow. The last column is the stability ratio, (S. R.), which is an

Table 1 Flow-induced vibration analysis results for YGN 3/4 steam generator.

Location of Entrance Flow	f_n Hz	V_{max}^* ft/sec	V_{ref} ft/sec	V_{cr} ft/sec	S.R. ⁽¹⁾
Cold Side Recirculation Fluid Entrance	135	6.4	4.2	5.9	0.71 (0.45) ⁽²⁾
Cold Side Feedwater Entrance	282	4.6	3.4	12.3	0.28 (0.43) ⁽²⁾
Hot Side Recirc. Fluid Entrance	207	8.2	7.0	9.5	0.73 (0.68) ⁽²⁾

Notes:

(1) S. R. = Stability Ratio = V_{eff} / V_{cr}

(2) C. E. results

indicator of tube susceptibility to potentially damaging flow-induced vibrations. The onset of instability occurs as S. R. approaches 1.0. The results of this analysis for YGN 3/4 shows that the design goal is met for all three critical regions of cross flow.

Based on the results of the Yonggwang 3/4 steam generator secondary fluid flow distribution analysis and subsequent tube bundle flow induced vibration evaluation, the predicted levels of tube vibration are sufficiently small that no unacceptable tube vibration or tube wear is anticipated.

References

- Beard, N. L., 1988, "Flow Induced Vibration Analysis," *CE Report*, CENC-1838.
- Connors, H. H., 1980, "Fluid Elastic Vibration of Tube Arrays Excited by Nonuniform Cross Flow," *Flow-Induced Vibration of Power Plant Components*, PVP-41.
- Hiestand, J. W. and Thakkar, J. G., 1984, "ATHOS and FLOW3 Simulation of the FRYING Heated Rod Bundle Experiment," *EPRI Report*, EPRI-NP-3514.
- Singhal, A. K., 1982, "ATHOS-A Computer Program for Thermal-Hydraulic Analysis of Steam Generators. Volume 1: Mathematical and

Physical Models and Methods of Solution, Volume 2: Programmer's Manual, Volume 3: User's Manual," *EPRI Report*, EPRI-NP-2698-CCM.

Swanson Analysis System Inc., 1992, "ANSYS Finite Element Computer Code."

Tatone, O. S. and Pathania, R. S., 1984, "Steam Generator Tube Performance: Experience with Water-Cooled Nuclear Power Reactors During 1982," *Atomic Energy of Canada Limit Report* AECL-8268.